**Showcasing Research from the Sustainable Materials Chemistry (SUSMATCHEM) research group at Stockholm University, Sweden.**

Organic solvent-free production of colloidally stable spherical lignin nanoparticles at high mass concentrations

A simple method was developed for the preparation of lignin nanoparticles and nanogels using the common lignin grades on the market. The approach avoids the use of organic solvents and allows high-consistency processing of lignin, thus significantly reducing water consumption and paving the way for a scalable production of lignin nanoparticles, gels and products thereof.

As featured in:
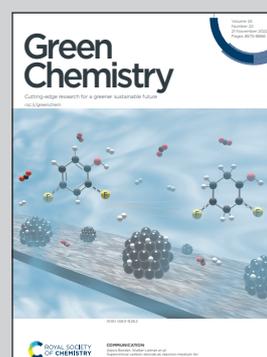
See Ievgen Pylypchuk and Mika H. Sipponen, *Green Chem.*, 2022, **24**, 8705.

ROYAL SOCIETY OF CHEMISTRY

rsc.li/greenchem

PAPER

Check for updates

Organic solvent-free production of colloidally stable spherical lignin nanoparticles at high mass concentrations†

Ievgen Pylypchuk [ID] and Mika H. Sipponen [ID] *

Lignin nanoparticles have emerged during the past decade as well-defined and renewable nanomaterials for fundamental and applied research. However, the presently known methods for the preparation of lignin nanoparticles rely on the use of organic solvents and energy intensive water evaporation processes. Here we present organic solvent-free production of spherical lignin nanoparticles by neutralization of alkaline solution of poorly water-soluble lignins in the presence of sodium lignosulfonate. We show that by combining these two predominant technical lignins it is possible to achieve colloidally stable lignin nanoparticle dispersions at concentrations exceeding 30 wt%. We further demonstrate versatility of the process by using ethanol organosolv lignin, soda lignin, and lignosulfonates from different sources. The lignin nanoparticle dispersions exhibit shear-thinning behaviour and undergo gelation within well-defined pH and concentration regions. Such flowable lignin dispersions mark a breakthrough towards scalable processing of lignin towards sustainable bio-based chemicals and materials.

1. Introduction

There is a growing need for biobased materials and chemicals to break free from our dependency on fossil resources.[1] Lignin is one of the most promising renewable feedstock types owing to its unique aromatic structure, low degree of polymerisation, and availability in the million-ton scale from the pulp and paper and biorefinery industries.[2] Nature has engineered lignin to provide plants with barrier properties, mechanical strength, and resistance against microbial and insect attacks. Owing to its biodegradability lignin is also circular in nature and provides a long-lasting carbon source to soils.[3]

Lignin is dissolved from plant biomass by cooking in aqueous solvents, and is typically considered as a byproduct, fuel, or waste in the pulping processes, depending on their technological maturity and production scale. Modern pulping processes have the ability isolate lignin without disturbing the closed-cycle chemical recovery processes. Today, lignosulfonates and kraft lignin dominate the lignin production with isolated quantities exceeding 1 Mt and 0.2 Mt every year. However, much more lignin could be isolated for the production of biobased materials and chemicals provided that the added value exceeds the investment and operation costs

involved. This problem of limited market supply asks for development of functional and high-value materials[4,5] in parallel with high-volume lignin formulations.[6] The commercial success of lignosulfonates as dispersing agens and binders in versatile end-uses originates from their water-solubility and ability to act as macromolecular surfactants. In contrast, poorly water-soluble kraft lignins are heterogeneous and structurally complex macromolecules with low molecular weight (about 5 kDa) and high dispersity. These attributes shared by many other lignin types seriously hinder their processing and formulation into biobased materials.[7]

Colloidal technology has emerged within the past ten years to overcome solubility and heterogeneity problems of poorly water-soluble lignins.[8–11] There have been many pioneering studies on the production of spherical lignin nanoparticles (LNPs) from various different lignin grades including kraft lignins, organosolv lignins, and soda lignins using "dry" and "wet" processes as recently reviewed.[12] Despite ongoing efforts to scale up these production processes there are serious obstacles that need to be overcome. For instance, so-called solvent exchange methods generate LNPs by dissolving lignin in water-miscible organic solvent and trigger aggregation of lignin by increasing the volume fraction of water. However, techno-economic assessments have shown that solvent recovery is the economical hot spot that accounts for the majority of the production cost.[13–15] Moreover, the upper ceiling for the concentration of LNPs that can be produced as colloidally stable dispersions is about 1 wt% using the solvent exchange

Department of Materials and Environmental Chemistry, Stockholm University, SE-10691 Stockholm, Sweden. E-mail: mika.sipponen@mmk.su.se

method. The dry processes generally employ aerosol technology to evaporate solvent from nebulized lignin droplets and resulting in spherical nano-microparticles.[16,17] In summary, the prevailing problems restrict large-scale production and applications of lignin nano/microparticles, including the high transportation costs of dilute aqueous suspensions, high operation costs from the energy-intensive solvent removal, and risks involved in production, transportation, and handling of dry nano- and microparticle powders.

It has become evident that unconservative approaches are needed to solve the aforementioned challenges. In the manufacturing industry it is common to improve properties through additives which often result in rather complex formulations, as is clear by taking a look into the ingredient lists of personal care products for instance. In contrast, it is quite astonishing that despite the alternate properties offered by various different lignins, many groups have insisted solving the problem through purification of lignin. These approaches include for instance fractionation of lignin to produce purified grades better suited to specialty uses.[18–22] Such analytical procedures have without doubt enriched our understanding of the lignin structure and reactivity at the molecular level.[23,24] However, development of lignin admixtures as an attempt to produce materials with new and improved properties is lacking from the published literature.

In the present work, we show that water-soluble lignosulfonates (SL) can be combined with poorly water-soluble lignins to produce colloidally stable LNP dispersions. We show that industrialy produced softwood kraft lignin (SKL), ethanol organosolv lignin (OSL) and soda lignin (SL) give rise to stable LNPs when their alkaline solutions are neutralised in the presence of lignosulfonates. In contrast to the earlier methods relying on organic solvents, our method is completely aqueous. We show production of LNPs at markedly high concentrations above the gel point of the dispersion and feasibility to work at high consistencies reaching 50 wt%. We also provide electron microscopy evidence that the LNPs are essentially mixed micellar particles consisting of loosely packed SKL surrounded by amphiphilic LS molecules. This scalable method presents a synergistic combination of the two most common lignin grades to alleviate the problem of lignin stability and processability in high-consistency water suspensions.

2. Experimental

2.1. Chemicals and materials

Softwood kraft lignin (SKL, BioPiva 100, UPM, Finland), sodium lignosulfonate (DS10, Domsjö, Sweden), sodium lignosulfonate (LS Sigma, Sigma Aldrich, SKU 471038), hardwood (beech) organosolv lignin (OSL), soda lignin (SL, Protobind 2400, Switzerland), sodium hydroxide (VWR, Sweden), sulfuric acid (VWR, Sweden), hydrochloric acid (VWR, Sweden), and dialysis membrane (MWCO 12–14 kDa, Spectra/Por, Sigma Aldrich) were used as received. Lignin characterization data provided in Table S1.†

2.2. Preparation of colloidal lignin nanoparticle dispersions

LS/SKL and LS/OSL dispersions were prepared as follows. A mixture of lignin was dissolved in 2 M NaOH and the pH was adjusted by 2 M H_2SO_4. For instance, to prepare solution with LS/SKL ratio 5 : 1, 225 g of LS and 45 g of SKL (dry content) were mixed with 405 g of aqueous 2 M sodium hydroxide solution and stirred overnight. To a 120 mL of obtained suspension (pH 13.3), 38.9 mL of 2 M sulfuric acid was added dropwise until pH 4.3 was reached. The formed gel was used as prepared or transferred into a dialysis bag (MWCO 12–14 kDa) and dialyzed against deionized water until reaching pH 6.

2.3 Potentiometric and conductometric titration

Titration of lignin was performed according to the protocol reported in[25] with slight modifications. Briefly, 1 g of lignin mixed with 5 mL of 2 M aqueous sodium hydroxide solution and then 500 mL of DI water was added. After 15 minutes the solution was filtered using Ahlstrom-Munksjö filter paper. Solution was titrated with 1 M hydrochloric acid using a pH meter (FiveEasy F20, Metter-Toledo GmbH, Switzerland) and conductivity meter (SevenExcellence, Mettler Toledo, Switzerland).

2.4 Characterization of colloidal dispersions

2.4.1 Particle size and zeta potential. Zeta potential and particle size of the particles were determined by electrophoretic mobility and dynamic light scattering (DLS) methods using Zeta Sizer instrument (Malvern, UK). The measurements were performed for water-diluted LS/SKL dispersions at 25 °C.

2.4.2 Dynamic viscosity. Dynamic viscositites of lignin nanoparticle dispersions were measured using a rotational viscometer (Viscotech Myr VR 3000) with R2–R5 spindles. The shear rate was varied for extrapolation of zero-shear viscosity and determination of dynamic viscosities as a function of total lignin concentration and pH.

2.4.3 Electron microscopy. For Transmission Electron Microscopy (TEM), 2 μl of dialyzed nanoparticles solution was drop casted over TEM grid (200 mesh Cu grid with thin carbon film) for 2 hours. Accelerating voltage was 120 kV and emission current 63 mA. For cryo-TEM, an aliquot of the dispersion was diluted in deionized water, deposited over a TEM grid and frozen in liquid ethane. The images were obtained under cooling with liquid nitrogen at an accelerating voltage of 200 kV.

3. Results and discussion

The poor water solubility of kraft lignin has limited its large-scale applications, which has given rise to different methods to prepare colloidal lignin particles as homogeneous dispersions that can be more easily processed.[26–28] However, scalability of the existing methods is severely restricted due to energy-intensive drying, evaporation, and organic solvent recovery processes. To overcome these obstacles, we have developed an organic solvent-free method to prepare colloidal lignin par-

ticles at considerably higher consistencies than previously achieved. Our approach starts by dissolving sodium lignosulfonate (LS) together with a poorly water-soluble lignin such as softwood kraft lignin (SKL) or beech ethanol organosolv lignin (OSL) in aquoues alkali (Fig. 1). The sufficient alkalinity required to dissolve the two lignins is about pH 10. A solution of approximately 50–60 wt% of lignin (LS + SKL) can be prepared this way. After complete dissolution, the mixed lignin solution is adjusted to a slightly acidic pH in the range of pH 4–7, which depending on the lignin concentration gives rise to a free-flowing colloidal dispersion or a homogeneous gel as shown in Fig. 1. Regardless of its physical state (liquid or gel) the colloidal system remains stable and can be refridgerated at 4 °C for several weeks without solid–liquid phase separation. Intrigued by these initial observations we systematically studied different weight ratios and lignin concentrations to decipher their influence on the stability and properties of the colloidal gel dispersion.

## 3.1 Formation of stable dispersions and different lignin ratios

The lignin market is expanding due to increased efforts on the development of lignin-based materials and expected growth of the lignocellulosic biorefineries sector. Today, lignosulfonates and kraft lignin are the two major lignin grades in the market with annual production exceeding 1 Mt and 0.2 Mt, respectively. We therefore chose LS and SKL as representative lignins to study possible mass ratios required to produce stable colloidal dispersions of the two lignins. Neutralization of a mixed solution of lignin in aqueous sodium hydroxide solution was studied in a broad range of mass ratios of LS to SKL from 1 : 1 to 12.5 : 1, keeping the concentration of LS constant at 10 wt% in the initial solution. DLS analysis showed that LS : SKL mass ratios below 4 : 1 yielded unstable dispersions with aggregating particles while higher ratios produced stable dispersions with z-average particle sizes below 170 nm (Fig. 2a and d). Dispersions were considered stable if no visible precipitation was observed after 24 h at room temperature. The lowest particle size (81 nm) was obtained at the LS : SKL ratio of 5 : 1, which corresponds to the current market availability of these two technical lignins. We note that it is possible to replace SKL by other poorly water-soluble lignins such as organosolv lignin (Fig. 2b) or soda lignin (Fig. 2c) or lignins. In particular, when OSL was mixed with LS, a weight ratio of 2.5 : 1 sufficed to a give colloidally stable dispersion with partice size of 160 nm

(Fig. 2b and e). As observed with SKL, the mixed dispersion of LS : OSL showed the lowest particle size of 100 nm at a lignin ratio of 5 : 1. There is thus a well-defined working window to produce stable colloidal particle dispersions at LS : SKL ratios 4–7 while with OSL and SL the ratios range from 2 to 7. These values mean that relative to the total lignin concentration at least 20% SKL and 33% OSL or SL that are otherwise poorly water-soluble at pH ≤ 7 can be stabilized in homogeneous colloidal dispersions for further processing or formulation. As it turns out, these values are associated with markedly high total lignin concentrations of the dispersion mixture.
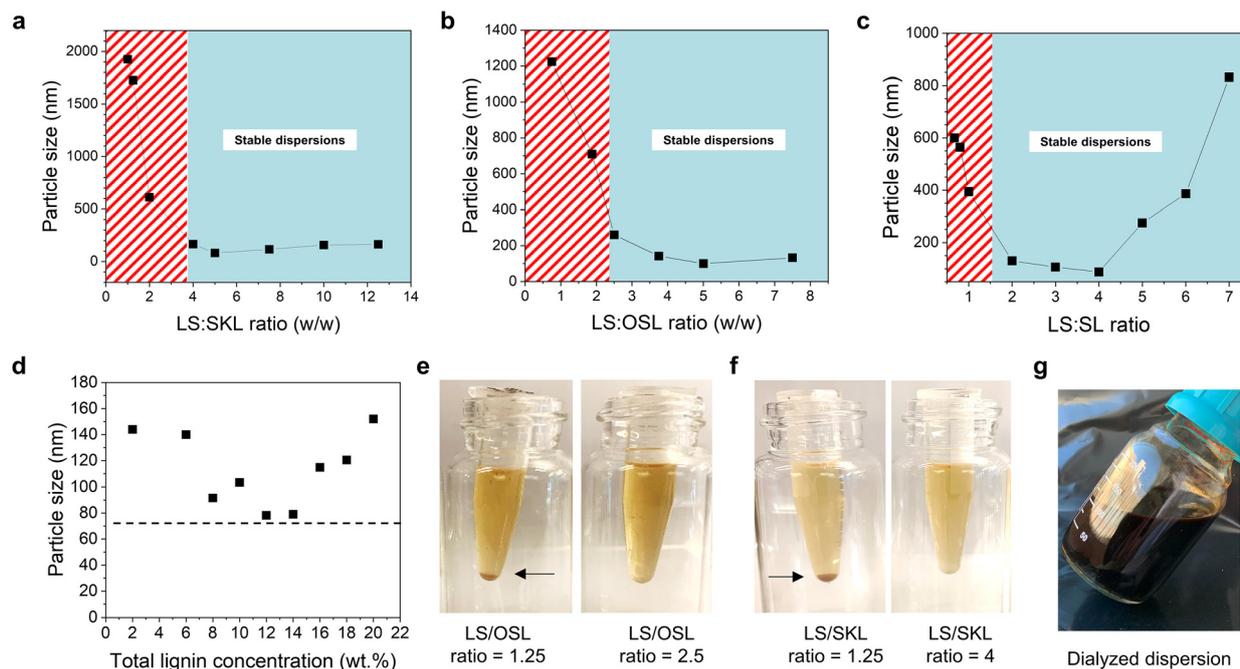
3.2 High-consistency colloidal dispersions

One of the major problems of previous aqueous–organic solvent-based methods has been the inability to prepare LNPs at industrially relevant concentrations above 2 wt% without drastically increasing the particle size and eventually agglomerating the entire system. Interestingly, we found that higher initial lignin concentrations lead to the formation of smaller LNPs. This trend is in stark contrast to the trend observed with colloidal particles prepared by solvent polarity shifting methods, where particle size increases as the lignin concentration increases.[14,29,30] In our method, the hydrodynamic diameter of the colloidal particles did not increase but decreased as the total lignin concentration increased from 2 wt% to 14 wt% at a 5 : 1 mass ratio of LS to SKL (Fig. 2e) as did the corresponding polydispersity indices (Fig. S1†). Moreover, we demonstrated that it is possible to purify the nanoparticle dispersion by dialysis against water while maintaining its colloidal stability (Fig. 2f). Our observations made it obvious that this new method of producing colloidal lignin particles can be operated at considerably high lignin concentrations above 20 wt%. The theoretical limit to the total lignin concentrations appears to be only restricted by the mutual solubility of the lignins in aqueous alkali. We were able to produce solutions containing 50 wt% of lignin at an LS : SKL ratio of 5 : 1 (Fig. S2†). At higher concentration of 63 wt% the mixture at a similar LS : SKL ratio had a paste-like appearance (Fig. S2†), which may necessitate extrusion processing to ensure homogeneous mixing with aqueous acid solution during the neutralization step.

We also noticed that some dispersions are more stable than others, and this trend was dependent on the lignin concentration. At 10–15 wt% total concentrations of lignin, the
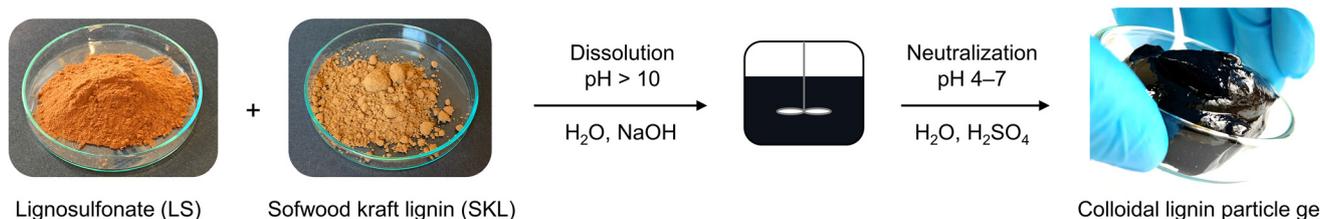
Fig. 1 Preparation of colloidal mixed micellar particle gels from sodium lignosulfonate (LS) and poorly water-soluble lignin such as softwood kraft lignin (SKL, pictured), beechwood ethanol organosolv lignin (OSL) or soda lignin (SL).

Diagram labels: Lignosulfonate (LS) + Sofwood kraft lignin (SKL) → Dissolution pH > 10, H₂O, NaOH → Neutralization pH 4–7, H₂O, H₂SO₄ → Colloidal lignin particle gel

Fig. 2 Effect of sodium lignosulfonate (LS) on particle size (hydrodynamic diameter, Z-average values based on DLS) and colloidal stability of lignin dispersions. Particle size of the dispersion as a function of mass ratio of (a) LS to softwood kraft lignin (SKL), (b) LS to beechwood organosolv lignin (OSL), and (c) LS to soda lignin. The initial concentration of LS was kept constant at 100 g L^{-1} while the concentrations of SKL, OSL and SL were varied and mixed in a 1:1 volume ratio with LS. (d) Particle size as a function of lignin concentration in the mixed colloidal dispersion at a constant LS to SKL ratio of 5:1 (w/w). Digital photographs of the diluted dispersions at weight ratios that produce unstable dispersions (the arrow indicate sedimentation) and colloidally stable dispersions at higher (e) LS/OSL and (f) LS/SKLdispersions. (g) Appearance of a dialyzed dispersion (LS:SKL 5:1 w/w) at a consistency of 12.4 wt%.

threshold ratio of LS to SKL can likely be lower than 4:1 as particle sizes below 100 nm were obtained in this region (Fig. 2c). These particles are smaller than those produced using organic solvent processes at considerably lower consistencies. For example, tetrahydrofuran:water (3:1 w/w) solvent system gives particles with average diameters of 200 to 400 nm at dispersion concentrations of about 0.5 wt% after evaporation of the organic solvent.[31] Acetone:water (3:1 w/w) solvent system is known to produce LNPs with smaller diameter than obtained from aqueous tetrahydrofuran,[32] but the working window for lignin concentrations is also lower. Moreover, despite its benefits and possible integration as a solvent in biorefinery processes, aqueous ethanol (50–70% by volume) limits the possible dispersion concentration of lignin to values below 0.3 wt%.[33,34] Therefore, this new particle production method not only avoids the use of volatile organic solvents, but also reduces water and energy consumption by a factor of 20–50 compared to the previously described methods.

As an attempt to understand this paradigm shift in lignin colloids, we can analyse differences in the solvent systems and their limiting lignin concentrations. According to the Stokes–Einstein equation, the translational diffusion coefficient is inversely proportional to the viscosity. Therefore, as viscosity increases the random collisions of colloidal particles becomes less frequent. In such a viscous system, lignin molecules have restricted mobility already in the initial solution. This limits

the particle formation space to a tighter domain, causing the formation of more dense-packed particles. This is confirmed by the fluorescence of LS-SKL dispersions, where the higher lignin concentrations resulted in a red-shift of fluorescence maxima, probably due to stronger π–π stacking interactions caused by denser molecular packing. This, in turn, results in so-called aggregation-induced fluorescence quenching (AIFQ) at higher concentrations (Fig. S3†). The AIFQ is a well-known phenomenon in systems where strong π–π interactions take place.[35] The blue shift of dialyzed LS-SKL nanoparticle dispersions (pH 6.3, λ_{max} = 400–450 nm) as compared to LS:SKL mixture in 2 M NaOH (pH 12, λ_{max} = 450–500 nm) confirms that charged lignin groups participate in π–π stacking, since their deprotonation at alkaline pH causes a shift in the electron density from aromatic rings of lignin, thus shifting their fluorescence maxima. Taking these theories together explains why high lignin concentrations give rise to increased stabilization of colloidal particles. In fact, such π–π stacking interactions are responsible for the supramolecular organization of sodium lignosulfonate in water solutions to form hollow micelles.[36]

3.3 Gelation and shear-thinning behavior

The ability to prepare colloidal lignin particles in markedly high consistencies intrigued us to determine their rheological properties that define their flowability and usability in many

practical applications. For simplicity, we maintained the weight ratio of LS to SKL constant at 5 : 1 and altered the total lignin concentration and pH as these are the two key parameters affecting the viscosity of the system. Based on the increase in viscosity in the order of one magnitude when the total lignin concentration was systematically increased, we can identify that at pH 5.5 the dispersion system undergoes gelation within a relatively narrow concentration region between 25 and 27 wt% (Fig. 3a). This kind of gelation behaviour marks a typical transformation from freely dispersed polymer particles to a solid-like state when crossing the percolation threshold, which is the point at which discrete nanoparticles form a continuous network that spans the entire gel volume.[37] Such interparticle bonds are non-covalent ones, and their formation is dependent on the pH, allowing us to conclude that they are hydrogen bonds, hydrophobic interaction forces, and van der Waals forces. Moreover, the drop in zero-shear viscosity occurred close to the apparent pK_a of the carboxyl

groups of the two kinds of lignins present (SKL, pK_a (–COOH) = 4.4; LS, pK_a (–COOH) = 4.0).[38,39] We can thus postulate that protonated carboxylic acid groups facilitate the formation of hydrogen bonds between the LNPs, whereas at pH > 5 they remain ionized and contribute to the excluded volume effect, while also counteracting interparticle depletion forces due to the electrostatic repulsion between the LNPs. Such a concentration-dependent gelation and direct preparation of LS-SKL nanoparticle gels is in contrast to our earlier observations with compact lignin nanoparticles, which are troublesome to concentrate from their original dilute dispersions to concentrations exceeding 3 wt%.[40]

As anticipated from the presence of acidic functional groups in the two lignins, variations in pH had a defining effect on the dynamic viscosity of their mixed colloidal dispersions (Fig. 3b). The lowest viscosities were measured from the solution at pH 9.9 which responded to shear like a dilatant fluid, *i.e.*, with viscosity increasing with increasing shear rate.
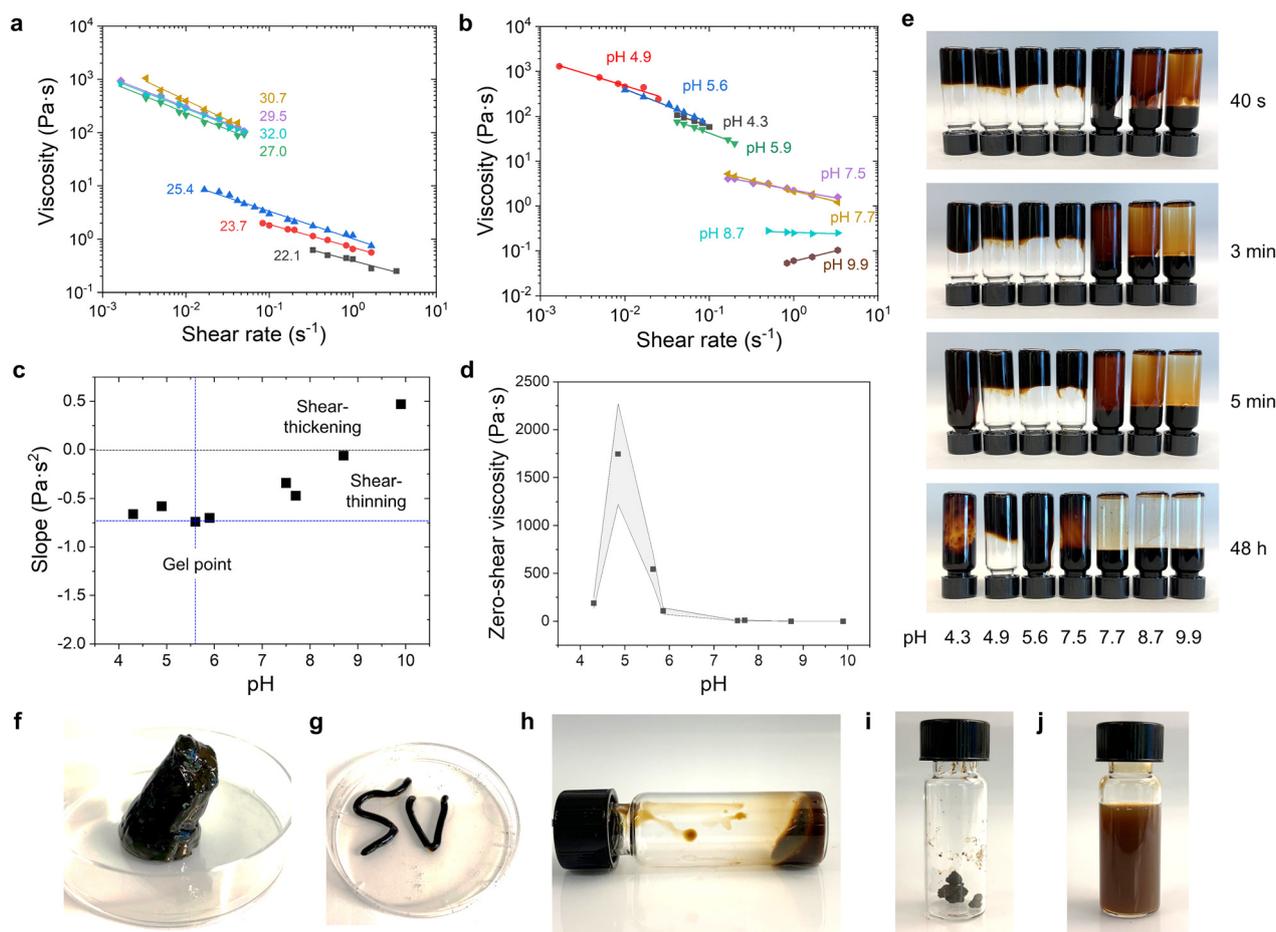
Fig. 3 Rheological properties and appearance of colloidal lignin gels. Dependency of dynamic viscosity of LS-SKL (5 : 1 w/w) dispersion on (a) total lignin concentration, expressed as wt%, while maintaining a constant pH 4.8 ± 0.5, and (b) dispersion pH 4.3–9.9 at a constant consistency of 32 wt%. (c) Mapping the rheological behaviour of the dispersion and estimation of the gel point from the slopes of linear fits to the data in (b) and (d) zero-shear viscosities as a function of pH. (e) Appearance and time-dependent flow behaviour of LS-SKL gel at 32 wt% consistency. (f) Appearance of the free-standing gel at 32 wt% concentration and demonstration of its (g) printability (the diameter of the Petri dish is 5.5 cm). LS + OS gel at 19 wt% consistency (h) and (i) after drying to ~90% dry content; and (j) after redispersing in water to a consistency of ~4 wt%.

There was a turning point in the fluid at pH 8.7 whereafter all the dispersions at lower pH values responded like pseudoplastic fluids, with shear-thinning behaviour. As indicated by major variations in dynamic viscosities, the pH region between pH 4–6 turned out important to define the rheological properties of the dispersion. When the linear fits to the logarithms of dynamic viscosities were plotted as a function of pH we can appreciate a gel point at approximately pH 5.6 (Fig. 3c). Fitted viscosity-shear rate curves are presented in Fig. S4† and were used for the extrapolation to estimate the corresponding zero-shear viscosities. The zero-shear viscosity increased as the pH was decreased, with a maximum at pH 4.9 (Fig. 3d). This pH-dependent viscosity behavior follows that of SKL but differs from that of LS present alone in solution.

Sodium lignosulfonate solution at 54 wt% concentration has been shown to respond to shear as a pseudoplastic fluid, with highest apparent viscosities at pH range 8.7–10.3 due to ionization of phenolic hydroxyl groups, thus causing stronger electrostatic repulsion both between the molecules and on the intramolecular level.[41] The latter causes the stretching of the hydrophobic chains of LS and their exposure.[42] Thus, in the LS-SKL mixture at alkaline pH > 9, the stretching of hydrophobic moieties of LS makes them more exposed to the solution and facilitates the formation of non-covalent bonds with SKL. This complexation stabilizes expanded LS molecule conformation, counteracting the coil-globule transition as the pH decreases. Further protonation allows for an increase in the level of non-covalent hydrogen bonding between the LS-SKL complexes, which triggers the formation of NPs at pH < 7.5. The intra- and intermolecular interactions of the two lignins

also lend explanation to the fact that the viscosity drops from pH 4.9 to 4.3. This is the pK_a region of carboxylic acids that when protonated no longer contribute to the repulsive forces, which may cause shrinking of the particles due to increased hydrogen bonding interactions. In agreement with the viscosity results, we observed that the dispersion at pH 4.9 showed very slow flowability in contrast to that observed at pH 4.3 (Fig. 3e).

This uncomplicated way to prepare shear-thinning lignin nanoparticle gels may open up new opportunities for example in three-dimensional printing. Intrigued by this opportunity, we observed time-dependent free-standing properties of the gel (Fig. 3f) and demonstrated injection of the gel using a 6 mL piston syringe (Fig. 3g). Another central consideration regarding applications is the ability to concentrate, dry and redisperse the particle dispersions. We found by using an LS-OSL dispersion as an example (Fig. 3h) that it is possible to air-dry the dispersion up to a 90% dry content (Fig. 3i), which ensures that the particles can be redispersed to a colloidal state (Fig. 3j). Therefore, such a colloidal lignin dispersion that can be transported in nearly dry form and free of dusting offers obvious advantages compared to the existing lignin dispersions either in dilute form or dry powder states.

3.4 Morphology and soft nature of the particles

Importantly, the stability of the dispersions seems to be dependent not only on the particle size but also on the shape of the particles. As can be seen from the TEM micrograph in Fig. 4a, a stable sample synthesized at an LS/SKL ratio of 5 : 1 was represented by spherical nanoparticles (average diameter of 26 ±
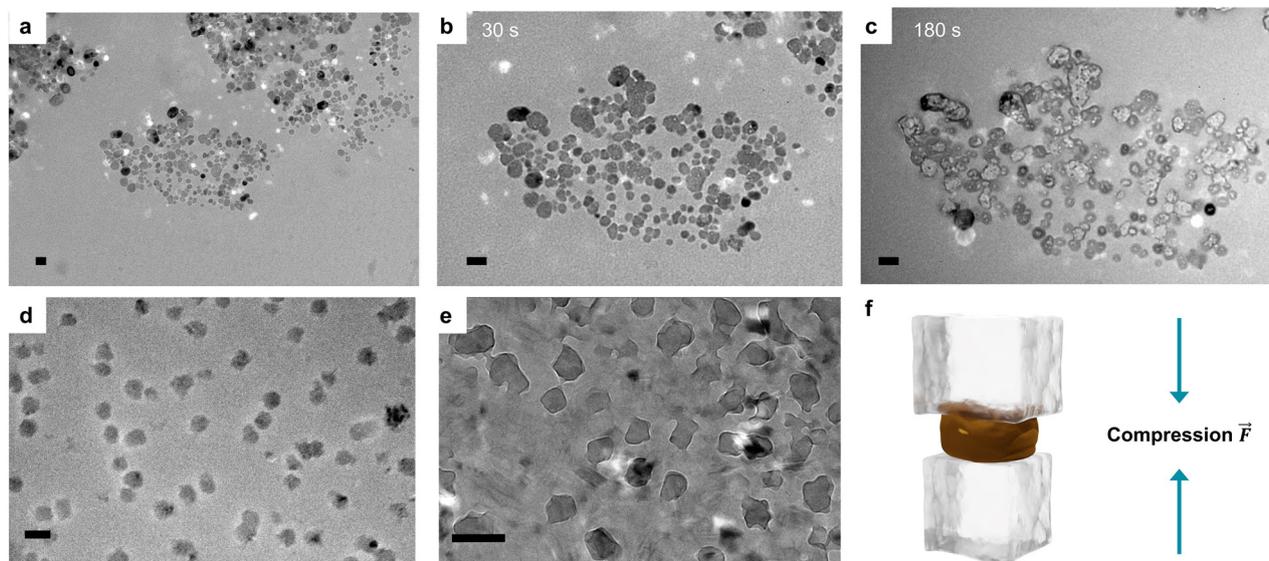
Fig. 4 Transmission electron microscopy (TEM) images of LS + SKL colloidal dispersion (5 : 1 w/w). (a) Regular TEM image at low magnification. Imaging at higher magnification, revealing beam-sensitivity of the particles after exposure of the same spot for (b) 30 seconds and (c) 180 seconds at 120 kV and emission current 63 mA. (d and e) Cryo–TEM micrographs recorded at −183 °C at an acceleration voltage of 200 kV. (f) Schematic illustration of the compression and deformation of the colloidal particle caused by water freezing under cryoscopic conditions (not drawn to scale). All scale bars: 100 nm.

9 nm according to image analysis, $N = 100$), while the precipitating samples consisted of non-spherical lignin aggregates (Fig. S5†). Moreover, unlike the particles prepared by solvent exchange processes, the spherical nanoparticles presented herein were found beam-sensitive, undergoing visible disintegration under extended times of beam exposure, as shown in Fig. 4b and c. Moreover, it was possible to observe the movement of matter inside the LNPs under 120 kV beam exposure. This makes us postulate that the particles are loosely packed micellar polyelectrolyte complexes stabilized by hydrophobic interactions in competition with repulsive electrostatic interactions of the sulfonate groups of LS. Similar effect was observed by Gorantla *et al.* when fullerene was moving along carbon nanotube due to the presence of weak non-covalent binding forces (π–π stacking).[43] We speculate that such kind of non-covalent interaction takes place in our LNPs as well. In a modeling study confirmed by TEM the formation of spherical micelles from sodium lignosulfonate was only possible when sodium benzene sulfonate (SBS) was added.[44] SBS seemed to stay inside the micelles, while LS molecules remained in the outer layer. A similar effect of stabilization due to intermolecular π–π stacking and hydrogen bonding was observed in our work, when the presence of SKL stabilizes the LS NPs. This makes us believe that the LS-SKL particles are stabilized by physically entangled and microphase-separated LS molecules, which prevents close packing of the two kinds of lignins in contrast to LNPs prepared by the solvent shifting method.[45] The low-energy intermolecular forces such as π–π stacking interactions and hydrogen bonds are perturbed under electron beam exposure, which leads to the observed changes in their nanoscale morphology. To provide further support for this theory, we also performed cryo-TEM imaging. As can be seen from Fig. 4d and e, the formation of ice crystals deformed the nanoparticles proving their softness. We anticipate that such a deformation results from thermal expansion of freezing water that non-uniformly compresses the particles in the ice matrix (Fig. 4f). Such a soft nature of these new all-lignin nanoparticles may prove useful for the development of new products with properties unavailable with the previously developed lignin colloids.

More precise description of particle formation as a function of pH is necessary to fundamentally understand the particle formation process and gain practical control over it. We determined particle size distributions (Fig. 5a) and plotted the number-based average particle sizes (Fig. 5b) at various pH values that correspond to viscous solutions and colloidal dispersions with nearly pH-independent appearance of black nanodispersions (Fig. S6†). Such optical properties of lignin nanoparticles are associated with particle sizes below 100 nm above which the dispersion becomes turbid. Such a change from dark brown solution to a yellow-brown turbid suspension is very well known to occur when alkaline kraft lignin solution is adjusted from pH 10 to pH 5. However, in the presence of lignosulfonate the particle size of lignin did not grow beyond the aforementioned threshold.

DLS analysis of the mixed lignin solution at pH 9.9 showed a peak centered at about 130 nm, indicating the presence of
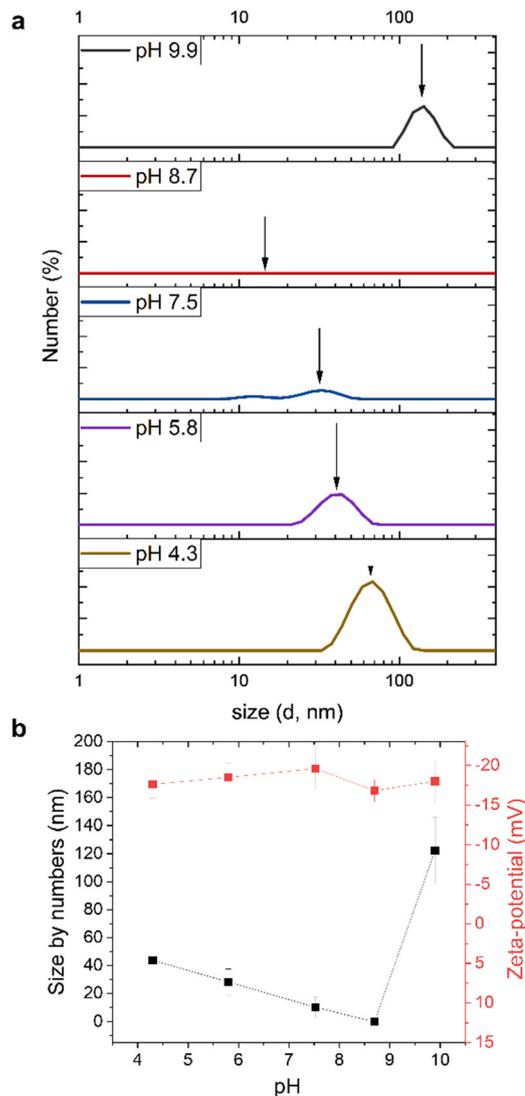

Fig. 5 pH-Dependency of particle size of LS : SKL mixed dispersion at a concentration of 32 wt% and at a ratio of LS to SKL of 5 : 1 (w/w). (a) Particle size distributions (by number) in the colloidal size range. (b) Change in the number-average particle size and zeta-potential as a function of pH.

larger micellar particles that may originate from LS. On the other hand, due to the prevailing high lignin concentration it is possible that solubility of SKL became critical and contributed to the formation of these micrometer sized micelles (Fig. 5b). To rule out a possible formation of aggregates during the sample dilution to DLS analysis, we measured the same samples by preparing dilutions in deionized water and in water adjusted to the corresponding pH values. There were no marked deviations in the particle size distribution curves, indicating that the particles were present in the original solutions and were unaffected by the dilution process. In fact, the ability of LS to form micelles in aqueous solutions is documented in the literature.[46] Qiu and co-workers showed by electron

microscopy of frozen samples that sodium lignosulfonate forms hollow vesicular micelles in water solution. The diameters of the micelles ranged from 500 nm to 1 μm, which means they were smaller than the major peak in the DLS-based size distribution present in our mixed lignin solutions. This difference is likely caused by the considerable higher concentration of LS used in the present study (27 wt%) and differences in purity and molecular weight distributions compared to those of Qiu *et al.* (membrane-fractionated sodium lignosulfonate at concentrations of 0.1 to 0.5 wt%).

Titration of lignin was made to understand which groups are available in aqueous solution upon pH precipitation. Potentiometric and conductometric titration curves are presented in Fig. S7–S9. The equivalence points corresponding to the start of the protonation of the phenolate anion and when the excess hydrochloric acid is present in the solution, were defined as V1 and V2 correspondingly.

As determined by titration, SKL has 4.09 mmol g^{-1} (defined as Ph-OH + COOH), and LS possesses 3.45 mmol g^{-1} of groups (defined as Ph-OH and SO$_3$H), LS/SKL mixture (mass ratio 5 : 1) has 4.12 mmol g^{-1} of OH groups. Taking into account the number of groups found by titration, the SO$_3$H can be estimated as 1.89 mmol g^{-1} (total acidic groups minus phenolic and carboxylic OH). It seems that SKL and LS/SKL in an aqueous solution possesses more charged groups than LS alone. These results can be compared to ^{31}P NMR studies, where the amount of Ph-OH for SKL was found to be 4.21 mmol g^{-1}, and 0.83 for LS (Table S1†). The total available hydroxyl content of the LS/SKL mixture is higher than the sum of individual contributions from both components. This is most probably due to aforementioned non-covalent LS-SKL interactions, allowing the LS backbone, stabilized by SKL, to be more expanded towards the solution and thus allowing charged groups to interact with solvent at lower pH, which was not possible in the absence of the LS-SKL complex.

Putting together the results discussed above allowed us to suggest a schematic mechanism for the formation of colloidal lignin nanoparticles of mixed lignin types (Fig. 6). From a process economy point of view it would be beneficial to minimize the use of acid and base for pH adjustment. Owing to the alkali-solubility of the majority of technical lignin grades, pH 10 seems like a reasonable starting point for making a solution mixture of two or more lignins. In the system of LS-SKL the lignosulfonate typically possesses a molecular weight of 50 kDa, *i.e.*, one magnitude higher than that of SKL (5 kDa).[47] Upon neutralization, SKL as well as other poorly water-soluble lignin grades are likely to precipitate and form spherical nuclei that begin to associate with LS chains. Compared to anionic polymeric flocculants with a typical molecular weight of 1–10 million daltons[48] LS have a relatively low molecular weight that in contrast to flocculation ensures formation of spherical micelles that are stabilized by the sulfonate groups. Although present in minority compared to the sulfonates and directly affected by the prevailing pH, the deprotonated carboxylic acid groups likely contribute to the anionic charge and lignin-lignin electrostatic repulsion that maintains the loosely packed micellar structure.

3.5 Water economy of the process

Regular laboratory procedures produce LNPs at mass concentrations of 0.2 to 1 wt%, and only a few examples exist of higher concentrations reaching about 3 wt%. To assess potential energy saving features of the present colloidal lignin dispersions one can consider a case where in order to save transportation costs the dispersion is concentrated to a consistency of 90 wt% by evaporating water. The energy consumption related to water evaporation is directly proportional to the concentration of dispersed solids. As can be seen from Table 1, the organic-solvent free method herein presented ensures that the amount of water to be removed is reduced by a factor 30–500, as compared to ordinary LNPs.
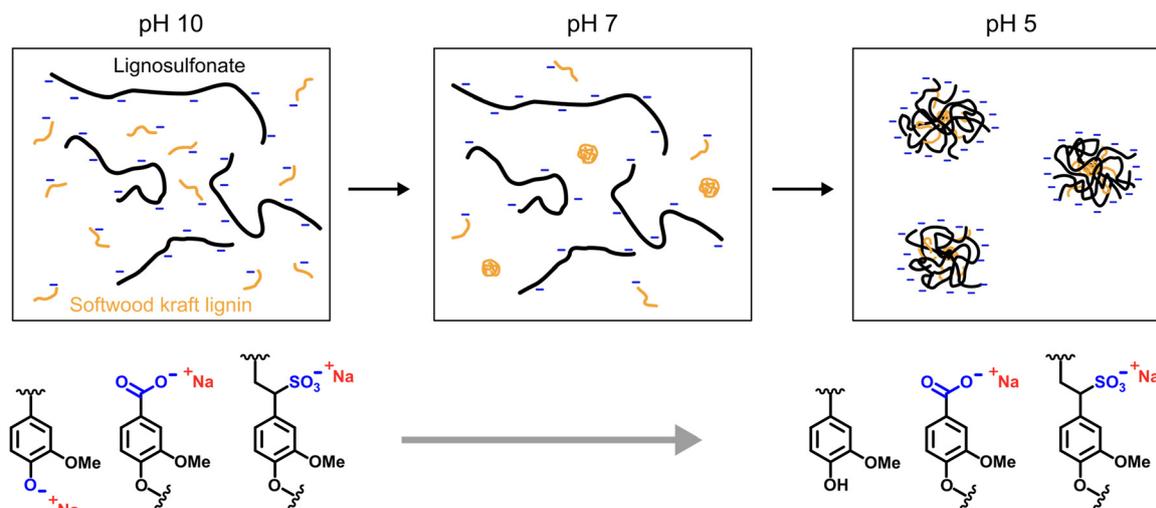

Fig. 6 Schematic model of formation of mixed micellar particles of lignosulfonate in the presence of softwood kraft lignin or other lignin poorly soluble below neutral pH.

Table 1 Comparison of mass balances and energy factors for evaporation of colloidal lignin particle dispersions with different initial mass concentrations

Composition of initial lignin dispersion				Evaporation to 90 wt% solids concentration			
Conc. LNPs wt%	Water content wt%	Mass of dispersion required for 100 kg dry substance kg	Water in initial dispersion kg	LNPs kg	Water in 90% dispersion kg	Water to be evaporated kg	Energy factor[a]
0.2	99.8	50 000	49 900	100	11.1	49888.9	561.3
1	99	10 000	9900	100	11.1	9888.9	111.3
3	97	3333	3233	100	11.1	3222.2	36.3
20	80	500	400	100	11.1	388.9	4.4
50	50	200	100	100	11.1	88.9	1.0

[a] Ratio of the amount of water evaporated relative to the amount in the case of 50 wt% lignin dispersion (this work).

4. Conclusions

We have presented a new facile method to prepare colloidal lignin dispersions at high consistencies exceeding 30 wt%. This method builds on contrastive aqueous solubility properties of two lignins in their mixtures. We used sodium lignosulfonate as a water-soluble lignin grade that was dissolved with softwood kraft lignin, beech wood ethanol organosolv lignin or soda lignin in aqueous alkali. We showed that colloidally stable nanoparticle dispersions can be produced by addusting the pH to neutral or mildly acidic pH 5. We put forward two main arguments in support of such an unorthodox mixing of different lignin grades. Firstly, the mass ratios needed to produce colloidally stable lignin dispersions satisfy the current market availability of lignosulfonates, softwood kraft lignin and other commercially available lignins. Our perspective is that this new particle process may be integrated to lignin recovery processes in existing sulphite and sulfate pulping units or combined with emerging biorefineries. Secondly, the unexpected material properties of the produced colloidal gels and especially their shear-thinning behaviour at high consistencies open new possibilities for the development of bio-based material formulations such as 3D printing inks, filaments, and porous materials in which lignin can play a major role in the future.

Author contributions

The authors conceptualized the work through equal contributions. I. P. was responsible for methodology, formal analysis, investigation, and validation. M. H. S. was responsible for visualization, resources, and supervision. M. H. S wrote the original draft with input from I. P. Both of the authors contributed to the writing – review & editing and approved the final version of the manuscript.

Conflicts of interest

The authors declare that they have filed a Swedish patent application for the production of colloidal lignin dispersions and are co-owners of a startup company Lignoflow Technologies AB that has interest in exploitation of the results reported in this paper.

Acknowledgements

References

1 A. Vinod, M. R. Sanjay, S. Suchart and P. Jyotishkumar, Renewable and sustainable biobased materials: An assessment on biofibers, biofilms, biopolymers and biocomposites, *J. Cleaner Prod.*, 2020, **258**, 120978.

2 D. Kai, M. J. Tan, P. L. Chee, Y. K. Chua, Y. L. Yap and X. J. Loh, Towards lignin-based functional materials in a sustainable world, *Green Chem.*, 2016, **18**(5), 1175–1200.

3 P. K. Donnelly, J. A. Entry, D. L. Crawford and K. Cromack, Cellulose and lignin degradation in forest soils: Response to moisture, temperature, and acidity, *Microb. Ecol.*, 1990, **20**(1), 289–295.

4 A. Moreno and M. H. Sipponen, Lignin-based smart materials: a roadmap to processing and synthesis for current and future applications, *Mater. Horiz.*, 2020, 7(9), 2237–2257.

5 J. J. Kaschuk, Y. Al Haj, O. J. Rojas, K. Miettunen, T. Abitbol and J. Vapaavuori, Plant-Based Structures as an Opportunity to Engineer Optical Functions in Next-Generation Light Management, *Adv. Mater.*, 2022, **34**, 2104473.

6 P. Jędrzejczak, M. N. Collins, T. Jesionowski and Ł. Klapiszewski, The role of lignin and lignin-based materials in sustainable construction – A comprehensive review, *Int. J. Biol. Macromol.*, 2021, **187**(July), 624–650.

7 A. Duval and M. Lawoko, A review on lignin-based polymeric, micro- and nano-structured materials, *React. Funct. Polym.*, 2014, **85**, 78–96.

8 H. Stewart, M. Golding, L. Matia-Merino, R. Archer and C. Davies, Manufacture of lignin microparticles by anti-solvent precipitation: Effect of preparation temperature and presence of sodium dodecyl sulfate, *Food Res. Int.*, 2014, **66**, 93–99.

9 Y. Qian, Y. Deng, X. Qiu, H. Li and D. Yang, Formation of uniform colloidal spheres from lignin, a renewable resource recovered from pulping spent liquor, *Green Chem.*, 2014, **16**(4), 2156–2163.

10 M. Lievonen, J. J. Valle-Delgado, M. L. Mattinen, E. L. Hult, K. Lintinen, M. A. Kostiainen, *et al.*, A simple process for lignin nanoparticle preparation, *Green Chem.*, 2016, **18**(5), 1416–1422.

11 C. Frangville, M. Rutkevičius, A. P. Richter, O. D. Velev, S. D. Stoyanov and V. N. Paunov, Fabrication of environmentally biodegradable lignin nanoparticles, *ChemPhysChem*, 2012, **13**(18), 4235–4243.

12 M. Österberg, M. H. Sipponen, B. D. Mattos and O. J. Rojas, Spherical lignin particles: A review on their sustainability and applications, *Green Chem.*, 2020, **22**(9), 2712–2733.

13 R. P. B. Ashok, P. Oinas, K. Lintinen, G. Sarwar, M. A. Kostiainen and M. Österberg, Techno-economic assessment for the large-scale production of colloidal lignin particles, *Green Chem.*, 2018, **20**(21), 4911–4919.

14 K. Lintinen, Y. Xiao, R. Bangalore Ashok, T. Leskinen, E. Sakarinen, M. Sipponen, *et al.*, Closed cycle production of concentrated and dry redispersible colloidal lignin particles with a three solvent polarity exchange method, *Green Chem.*, 2018, **20**(4), 843–850.

15 C. Abbati de Assis, L. G. Greca, M. Ago, M. Balakshin, H. Jameel, R. Gonzalez, *et al.*, Techno-Economic Assessment, Scalability, and Applications of Aerosol Lignin Micro- and Nanoparticles, *ACS Sustainable Chem. Eng.*, 2018, **6**(9), 11853–11868.

16 M. Ago, S. Huan, M. Borghei, J. Raula, E. I. Kauppinen and O. J. Rojas, High-throughput synthesis of lignin particles (~30 nm to ~2 μm) via aerosol flow reactor: Size fractionation and utilization in pickering emulsions, *ACS Appl. Mater. Interfaces*, 2016, **8**(35), 23302–23310.

17 C. Abbati de Assis, L. G. Greca, M. Ago, M. Balakshin, H. Jameel, R. Gonzalez, *et al.*, Techno-Economic Assessment, Scalability, and Applications of Aerosol Lignin Micro- and Nanoparticles, *ACS Sustainable Chem. Eng.*, 2018, **6**(9), 11853–11868.

18 M. Gigli and C. Crestini, Fractionation of industrial lignins: opportunities and challenges, *Green Chem.*, 2020, **22**(15), 4722–4746.

19 R. E. Majdar, A. Ghasemian, H. Resalati, A. Saraeian, C. Crestini and H. Lange, Case Study in Kraft Lignin Fractionation: 'Structurally Purified' Lignin Fractions-The Role of Solvent H-Bonding Affinity, *ACS Sustainable Chem. Eng.*, 2020, **8**(45), 16803–16813.

20 C. Gioia, M. Colonna, A. Tagami, L. Medina, O. Sevastyanova, L. A. Berglund, *et al.*, Lignin-Based Epoxy Resins: Unravelling the Relationship between Structure and Material Properties, *Biomacromolecules*, 2020, **21**, 1920–1928.

21 M. Balakshin, E. A. Capanema, I. Sulaeva, P. Schlee, Z. Huang, M. Feng, *et al.*, New Opportunities in the Valorization of Technical Lignins, *ChemSusChem*, 2021, 57.

22 J. Behaghel De Bueren, F. Héroguel, C. Wegmann, G. R. Dick, R. Buser and J. S. Luterbacher, Aldehyde-Assisted Fractionation Enhances Lignin Valorization in Endocarp Waste Biomass, *ACS Sustainable Chem. Eng.*, 2020, **8**(45), 16737–16745.

23 N. Giummarella, I. V. Pylypchuk, O. Sevastyanova and M. Lawoko, New Structures in Eucalyptus Kraft Lignin with Complex Mechanistic Implications, *ACS Sustainable Chem. Eng.*, 2020, **8**(29), 10983–10994.

24 N. Giummarella, P. A. Lindén, D. Areskogh and M. Lawoko, Fractional Profiling of Kraft Lignin Structure: Unravelling Insights on Lignin Reaction Mechanisms, *ACS Sustainable Chem. Eng.*, 2020, **8**(2), 1112–1120.

25 L. Serrano, E. S. Esakkimuthu, N. Marlin, M. C. Brochier-Salon, G. Mortha and F. Bertaud, Fast, Easy, and Economical Quantification of Lignin Phenolic Hydroxyl Groups: Comparison with Classical Techniques, *Energy Fuels*, 2018, **32**(5), 5969–5977.

26 M. Österberg, M. H. Sipponen, B. D. Mattos and O. J. Rojas, Spherical lignin particles: A review on their sustainability and applications, *Green Chem.*, 2020, **22**, 2712–2733.

27 S. Beisl, A. Miltner and A. Friedl, Lignin from micro- to nanosize: Production methods, *Int. J. Mol. Sci.*, 2017, **18**, 1244.

28 W. Zhao, B. Simmons, S. Singh, A. Ragauskas and G. Cheng, From lignin association to nano-/micro-particle preparation: extracting higher value of lignin, *Green Chem.*, 2016, **18**(21), 5693–5700.

29 T. Leskinen, M. Smyth, Y. Xiao, K. Lintinen, M. L. Mattinen, M. A. Kostiainen, *et al.*, Scaling Up Production of Colloidal Lignin Particles, *Nord. Pulp Pap. Res. J.*, 2017, **32**(4), 586–596.

30 I. V. Pylypchuk, A. Riazanova, M. E. Lindström and O. Sevastyanova, Structural and molecular-weight-dependency in the formation of lignin nanoparticles from fractionated soft- And hardwood lignins, *Green Chem.*, 2021, **23**(8), 3061–3072.

31 T. Leskinen, M. Smyth, Y. Xiao, K. Lintinen, M. L. Mattinen, M. A. Kostiainen, *et al.*, Scaling Up Production of Colloidal Lignin Particles, *Nord. Pulp Pap. Res. J.*, 2017, **32**(4), 586–596.

32 T. Zou, N. Nonappa, M. Khavani, M. Vuorte, P. Penttilä, A. Zitting, *et al.*, Experimental and Simulation Study of the Solvent Effects on the Intrinsic Properties of Spherical Lignin Nanoparticles, *J. Phys. Chem. B*, 2021, **125**(44), 12315–12328.

33 M. H. Sipponen, H. Lange, M. Ago and C. Crestini, Understanding Lignin Aggregation Processes, A Case Study: Budesonide Entrapment and Stimuli Controlled Release from Lignin Nanoparticles, *ACS Sustainable Chem. Eng.*, 2018, **6**(7), 9342–9351.

34 D. Koch, M. Paul, S. Beisl, A. Friedl and B. Mihalyi, Life cycle assessment of a lignin nanoparticle biorefinery: Decision support for its process development, *J. Cleaner Prod.*, 2020, **245**, 118760.

35 X. Ma, R. Sun, J. Cheng, J. Liu, F. Gou, H. Xiang, *et al.*, Fluorescence Aggregation-Caused Quenching versus Aggregation-Induced Emission: A Visual Teaching Technology for Undergraduate Chemistry Students, *J. Chem. Educ.*, 2016, **93**(2), 345–350.

36 X. Qiu, Q. Kong, M. Zhou and D. Yang, Aggregation behavior of sodium lignosulfonate in water solution, *J. Phys. Chem. B*, 2010, **114**(48), 15857–15861.

37 R. A. L. Jones, *Soft condensed matter, Soft Condensed Matter*, Oxford University Press Inc., New York, 2002, pp. 196.

38 W. Zhu, *Equilibrium of Lignin Precipitation The Effects of pH, Temperature, Ion Strength and Wood Origins Equilibrium of Lignin Precipitation*, Vol. **46**, Licenciate Thesis, Chalmers University of Technology, 2013.

39 R. Li, D. Yang, W. Guo and X. Qiu, The adsorption and dispersing mechanisms of sodium lignosulfonate on Al2O3 particles in aqueous solution, *Holzforschung*, 2013, **67**(4), 387–394.

40 K. Lintinen, Y. Xiao, R. Bangalore Ashok, T. Leskinen, E. Sakarinen, M. Sipponen, *et al.*, Closed cycle production of concentrated and dry redispersible colloidal lignin particles with a three solvent polarity exchange method, *Green Chem.*, 2018, **20**(4), 843–850.

41 Q. Tang, M. Zhou, D. Yang and X. Qiu, Effects of pH on aggregation behavior of sodium lignosulfonate (NaLS) in concentrated solutions, *J. Polym. Res.*, 2015, **22**, 50.

42 M. Yan, D. Yang, Y. Deng, P. Chen, H. Zhou and X. Qiu, Influence of pH on the behavior of lignosulfonate macromolecules in aqueous solution, *Colloids Surf., A*, 2010, **371**(1–3), 50–58.

43 S. Gorantla, S. Avdoshenko, F. Börrnert, A. Bachmatiuk, M. Dimitrakopoulou, F. Schäffel, *et al.*, Enhanced π-π interactions between a C60 fullerene and a buckle bend on a double-walled carbon nanotube, *Nano Res.*, 2010, **3**(2), 92–97.

44 G. Zhu, G. Yin, J. Ding, Q. Tang, J. Shang and X. Lin, Sodium Benzenesulfonate-Assisted Preparation of Lignosulfonate-Based Spherical Micelles: Insights from Mesoscopic Simulations, *ACS Sustainable Chem. Eng.*, 2022, **10**(6), 2262–2270.

45 T. Zou, N. Nonappa, M. Khavani, M. Vuorte, P. Penttilä, A. Zitting, *et al.*, Experimental and Simulation Study of the Solvent Effects on the Intrinsic Properties of Spherical Lignin Nanoparticles, *J. Phys. Chem. B*, 2021, **125**(44), 12315–12328.

46 X. Qiu, Q. Kong, M. Zhou and D. Yang, Aggregation behavior of sodium lignosulfonate in water solution, *J. Phys. Chem. B*, 2010, **114**(48), 15857–15861.

47 M. H. Sipponen, M. Farooq, J. Koivisto, A. Pellis, J. Seitsonen and M. Österberg, Spatially confined lignin nanospheres for biocatalytic ester synthesis in aqueous media, *Nat. Commun.*, 2018, **9**, 1–7.

48 M. B. Hocking, K. A. Klimchuk and S. Lowen, Polymeric flocculants and flocculation, *J. Macromol. Sci., Rev. Macromol. Chem. Phys.*, 1999, **C39**(2), 177–203.